



ARL-TR-9048 • SEP 2020



# ALE3D-Magnetohydrodynamic Simulation of a Small Helical Magnetic Flux Generator

by George B Vunni and Anthony J Johnson

Approved for public release; distribution is unlimited.

## **NOTICES**

### **Disclaimers**

The findings in this report are not to be construed as an official Department of the Army position unless so designated by other authorized documents.

Citation of manufacturer's or trade names does not constitute an official endorsement or approval of the use thereof.

Destroy this report when it is no longer needed. Do not return it to the originator.



# **ALE3D-Magnetohydrodynamic Simulation of a Small Helical Magnetic Flux Generator**

**George B Vunni**

*Weapons and Materials Research Directorate, CCDC Army Research Laboratory*

**Anthony J Johnson**

*Lawrence Livermore National Laboratory*

**REPORT DOCUMENTATION PAGE**

*Form Approved*  
OMB No. 0704-0188

Public reporting burden for this collection of information is estimated to average 1 hour per response, including the time for reviewing instructions, searching existing data sources, gathering and maintaining the data needed, and completing and reviewing the collection information. Send comments regarding this burden estimate or any other aspect of this collection of information, including suggestions for reducing the burden, to Department of Defense, Washington Headquarters Services, Directorate for Information Operations and Reports (0704-0188), 1215 Jefferson Davis Highway, Suite 1204, Arlington, VA 22202-4302. Respondents should be aware that notwithstanding any other provision of law, no person shall be subject to any penalty for failing to comply with a collection of information if it does not display a currently valid OMB control number.

**PLEASE DO NOT RETURN YOUR FORM TO THE ABOVE ADDRESS.**

<b>1. REPORT DATE (DD-MM-YYYY)</b> September 2020		<b>2. REPORT TYPE</b> Technical Report		<b>3. DATES COVERED (From - To)</b> March–September 2020	
<b>4. TITLE AND SUBTITLE</b> ALE3D-Magnetohydrodynamic Simulation of a Small Helical Magnetic Flux Generator				<b>5a. CONTRACT NUMBER</b>	
				<b>5b. GRANT NUMBER</b>	
				<b>5c. PROGRAM ELEMENT NUMBER</b>	
<b>6. AUTHOR(S)</b> George B Vunni and Anthony J Johnson				<b>5d. PROJECT NUMBER</b>	
				<b>5e. TASK NUMBER</b>	
				<b>5f. WORK UNIT NUMBER</b>	
<b>7. PERFORMING ORGANIZATION NAME(S) AND ADDRESS(ES)</b> CCDC Army Research Laboratory ATTN: FCDD-RLW-PD Aberdeen Proving Ground, MD 21005-5066				<b>8. PERFORMING ORGANIZATION REPORT NUMBER</b>  ARL-TR-9048	
<b>9. SPONSORING/MONITORING AGENCY NAME(S) AND ADDRESS(ES)</b>				<b>10. SPONSOR/MONITOR'S ACRONYM(S)</b>	
				<b>11. SPONSOR/MONITOR'S REPORT NUMBER(S)</b>	
<b>12. DISTRIBUTION/AVAILABILITY STATEMENT</b> Approved for public release; distribution is unlimited.					
<b>13. SUPPLEMENTARY NOTES</b> ORCID ID(s): George Vunni, 0000-0002-7178-4899					
<b>14. ABSTRACT</b> The US Army Combat Capabilities Development Command Army Research Laboratory is actively engaged in both computational and experimental programs to design magnetic flux compression generators (FCGs) as pulsed power sources for protection applications. This report focuses on simulation of a similar helical FCG designed by Patrik Appelgren of the Swedish Defense Research Agency using the ALE3D magnetohydrodynamic (MHD) code developed by Lawrence Livermore National Laboratory. For this FCG device, the MHD simulation showed excellent agreement during the operation of the generator. The ALE3D-MHD model overpredicted the final current.					
<b>15. SUBJECT TERMS</b> magnetic flux compression generator, FCG, ALE3D, magnetohydrodynamics, pulsed power					
<b>16. SECURITY CLASSIFICATION OF:</b>			<b>17. LIMITATION OF ABSTRACT</b>  UU	<b>18. NUMBER OF PAGES</b>  23	<b>19a. NAME OF RESPONSIBLE PERSON</b> George B Vunni
<b>a. REPORT</b> Unclassified	<b>b. ABSTRACT</b> Unclassified	<b>c. THIS PAGE</b> Unclassified			<b>19b. TELEPHONE NUMBER (Include area code)</b> (410) 278-8538

## Contents

---

<b>List of Figures</b>	<b>iv</b>
<b>Acknowledgments</b>	<b>v</b>
<b>1. Motivation and Introduction</b>	<b>1</b>
<b>2. FCG Geometry</b>	<b>3</b>
<b>3. ALE3D Schuck Physics Code</b>	<b>4</b>
<b>4. ALE3D-MHD Simulation</b>	<b>4</b>
4.1 Geometry and Mesh	4
4.2 ALE3D Circuit Simulation Setup	6
4.3 Material Properties	7
<b>5. ALE3D-MHD Simulation Results</b>	<b>7</b>
<b>6. Conclusion</b>	<b>13</b>
<b>7. References</b>	<b>14</b>
<b>List of Symbols, Abbreviations, and Acronyms</b>	<b>15</b>
<b>Distribution List</b>	<b>16</b>

## List of Figures

---

Fig. 1	A cross section of the FOI FCG. A-initiator, B-seed current cables, C-crowbar ring, D-stator coil, E-return conductor, F-armature and G-high-explosive PBXN-5.....	2
Fig. 2	The current recordings in experiments with FCG #1 and FCG #2: a) pre-crowbar seed currents and b) output currents (plot is shifted at the point of crowbar contact). The double arrows indicate the approximate time interval during which the contact point is within a specific section.....	2
Fig. 3	Solid model of Appelgren helical FCG with 90° slice removed: a) without insulation materials and b) with insulation materials .....	3
Fig. 4	Computational mesh and simulation domain with 90° slice removed..	5
Fig. 5	a) Mesh of the FCG device and b) zoomed-in section of the FCG coil showing the number of elements .....	6
Fig. 6	ALE3D simulation setup showing the external circuit and the computational mesh .....	7
Fig. 7	ALE3D simulation geometry at a) crowbar time, b) end of section 1, c) end of section 2, d) end of section 3, e) end of section 4, and f) end of compression .....	8
Fig. 8	Pre-crowbar current plot from ALE3D simulation vs. experiment for FCG #1 and FCG #2 .....	9
Fig. 9	ALE3D MHD current vs. experiment: a) FCG #1 and b) FCG #2.....	11
Fig. 10	ALE3D MHD inductance vs. experiment for FCG #1 .....	12

## **Acknowledgments**

---

The author would also would like to thank Dr Patrik Appelgren, Deputy Research Director of the Swedish Defense Research Agency, for useful discussion during my visit to their pulsed power laboratory.

This work was supported in part by a grant of computer time from the Department of Defense High Performance Computing Modernization Program at the Army Research Laboratory Department of Defense Supercomputing Resource Center.

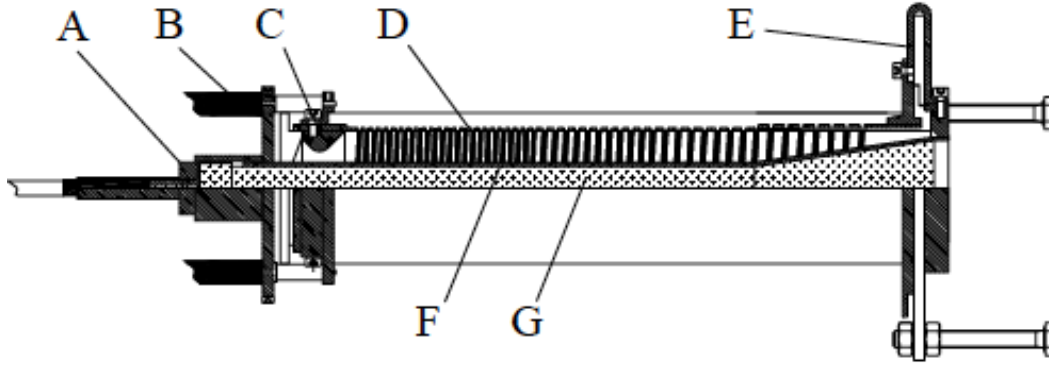
## 1. Motivation and Introduction

---

Numerical simulation is one of the tools used for detailed understanding of magnetic flux compression generators (FCGs) and a quantitative description of physical phenomena occurring during flux compression. The motivation of this simulation is to benchmark the ALE3D-magnetohydrodynamic (MHD) computational tool to predict the performance of a flux compression device designed and tested by Appelgren.<sup>1-4</sup> Modeling of this device will help us understand the performance of a similar FCG device developed at the US Army Combat Capabilities Development Command (CCDC) Army Research Laboratory.<sup>5-7</sup> As further motivation for modeling FCGs, magnetic simulation allows us to look at design details that are difficult to see experimentally, such as magnetic coupling, magnetic pressure effects, hot spots, eddy currents, and component imperfections. This report focuses on the ALE3D-MHD simulation of Appelgren's experiments.<sup>1,2</sup> Since the focus of this report is the MHD simulation, the details of the experiment are briefly summarized. A more detailed description of the Appelgren experiment can be found in the literature.<sup>1-4</sup>

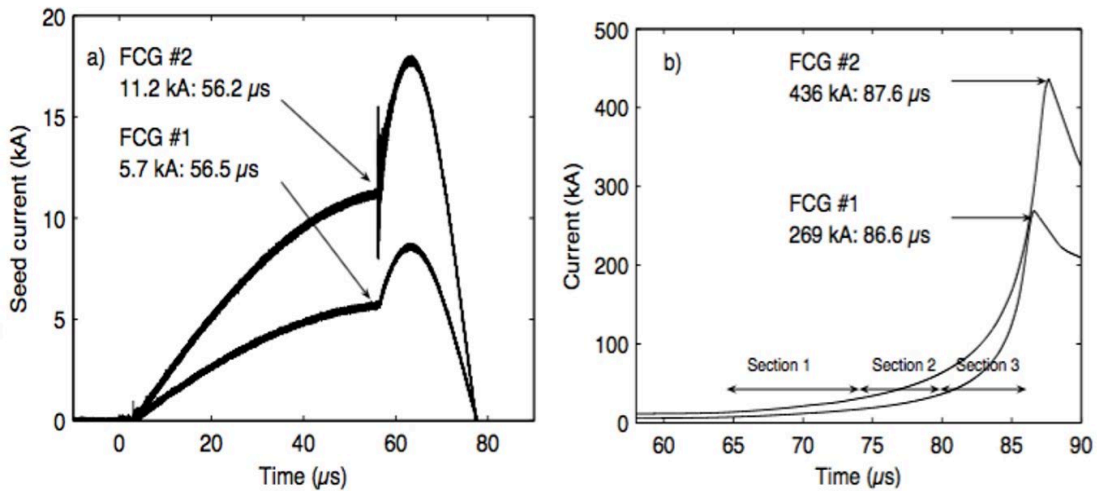
The helical FCG is a type of generator that consists of a conducting cylindrical coil (stator) and a coaxial, conducting cylindrical tube (armature) filled with high explosives. The coil is energized by a seed current, with a return path via the load and armature. When the explosive is initiated, the armature rapidly expands, trapping the magnetic flux in the shrinking volume between the coil and armature. As the detonation moves forward, the coil is shorted out turn by turn by the armature, resulting in the reduction of the circuit inductance and increase in the current.

Figure 1 shows a 3-D cross section of the helical FCG designed by Appelgren<sup>1,2</sup> at the Swedish Defense Research Agency (FOI).<sup>1</sup> Also shown in Fig. 1 are the different sections and some of the vital components of Appelgren's helical generator. The FCG device had an initial inductance of 23  $\mu\text{H}$  and a load of approximately 0.2  $\mu\text{H}$ . It was loaded with 0.27 kg of PBXN-5 explosive.



**Fig. 1** A cross section of the FOI FCG. A-initiator, B-seed current cables, C-crowbar ring, D-stator coil, E-return conductor, F-armature and G-high-explosive PBXN-5.<sup>1</sup>

In Appelgren's work, two sets of experiments were conducted. The first test (FCG #1) was seeded with a low seed current of 5.7 kA, and the second test (FCG #2) was seeded with a high current of 11.2 kA. The seed current was supplied by a 67- $\mu$ F capacitor bank charge at approximately at 4.2 and 8.0 kV. The generator was crowbarred just before the peak of the seed current occurring at around 56.5  $\mu$ s. The peak of the current was reached about 30  $\mu$ s after the time of crowbar. Final compressed currents of 269 and 436 kA were obtained, corresponding to current amplification factors of 47 and 39.<sup>1</sup> Figure 2 shows the seed and output current recordings for FCG #1 and FCG #2.<sup>1,2</sup>



**Fig. 2** The current recordings in experiments with FCG #1 and FCG #2<sup>1,2</sup>: a) pre-crowbar seed currents and b) output currents (plot is shifted at the point of crowbar contact). The double arrows indicate the approximate time interval during which the contact point is within a specific section.

## 2. FCG Geometry

Figure 3 shows a cutaway 3-D model of Appelgren's FCG without and with insulator material and illustrates the different sections of the helical generator. A coaxial input geometry was added for connecting the external seed current to better approximate the final impedance of the generator. The complete geometry was generated in Cubit using python script. The geometry may have simplifications compared to the physical generator reported in Appelgren.<sup>1</sup> Some geometric features still had to be estimated because of missing details from Appelgren thesis.<sup>1</sup> Each material component is exported as tetrahedral mesh that is used for shaping materials into ALE3D code.

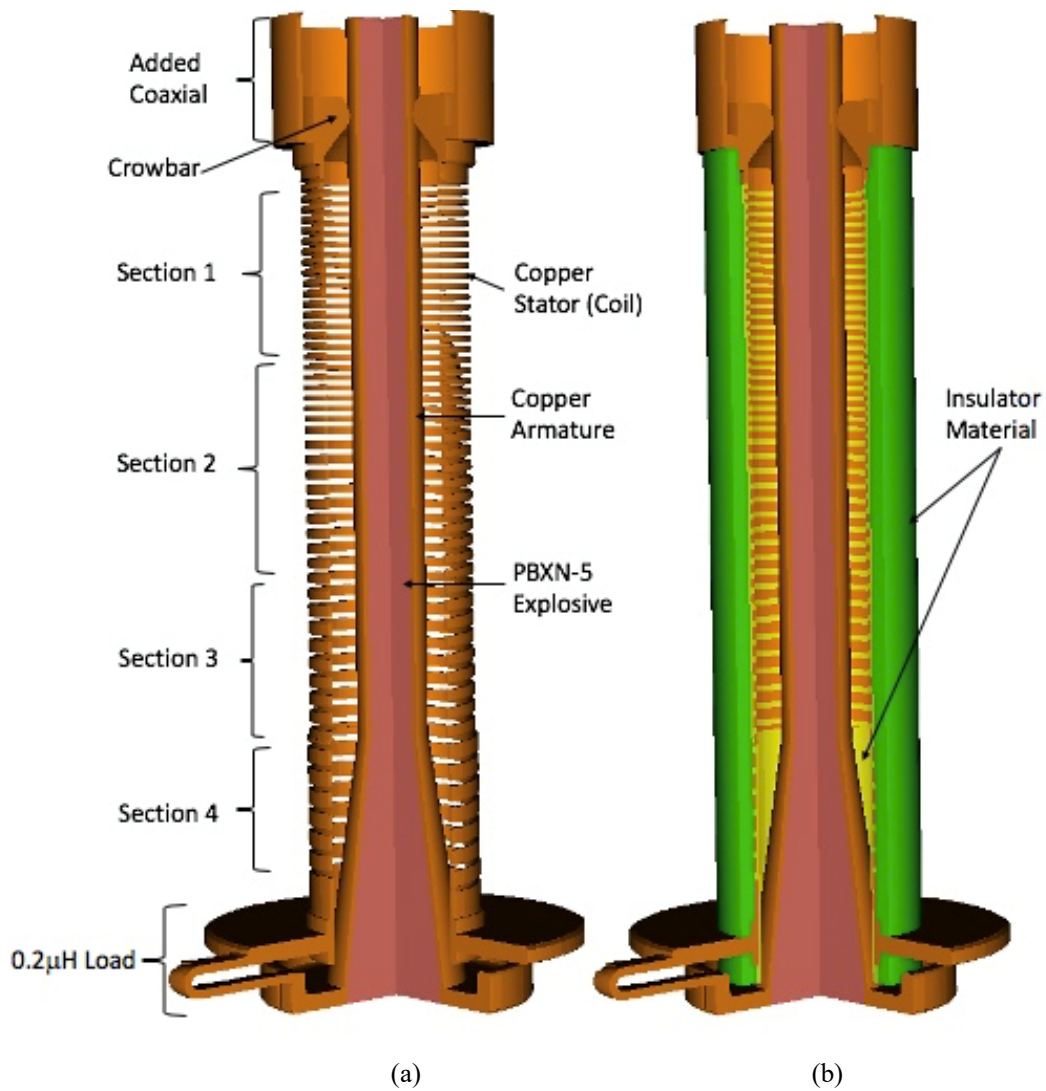


**Fig. 3** Solid model of Appelgren helical FCG with 90° slice removed: a) without insulation materials and b) with insulation materials

### **3. ALE3D Schuck Physics Code**

---

ALE3D is a multiphysics numerical simulation software tool using arbitrary Lagrangian–Eulerian (ALE) techniques.<sup>6</sup> ALE3D’s MHD model is capable of capturing the dynamics of electrically conducting solids and fluids. The MHD module was developed primarily for the modeling of coupled electro-thermal-mechanical systems that are inherently 3-D in nature. Example applications for this capability include explosively driven FCGs, induction heating, metal forming, and electromagnetic rail gun systems.

The ALE3D MHD module solves the resistive magnetic induction equation given a collection of specified current and voltage sources. The equation is solved in the Lagrangian frame using a mixed finite element method employing H (Curl) and H (Div.) finite element basis functions that preserve the solenoidal nature of the magnetic field to machine precision. Electromagnetic force and resistive joule heating terms are coupled to the equations of motion and thermal diffusion in an operator split manner. For problems that require mesh relaxation, magnetic advection is performed using the method of algebraic constrained transport that is valid for unstructured hexahedral grids with arbitrary mesh velocities. The advection method maintains the divergence-free nature of the magnetic field and is second-order accurate in regions where the solution is sufficiently smooth. For regions in which the magnetic field is discontinuous (e.g., MHD shocks), the advection step is limited using the method of algebraic flux correction as explained in detail in the ALE3D manual.<sup>5,6</sup>

### **4. ALE3D-MHD Simulation**

---

#### **4.1 Geometry and Mesh**

---

Figure 4 show a 3-D cutaway of the simulation domain. The mesh resolution was primarily set to resolve geometric features. The mesh consisted of approximately 6 million elements.

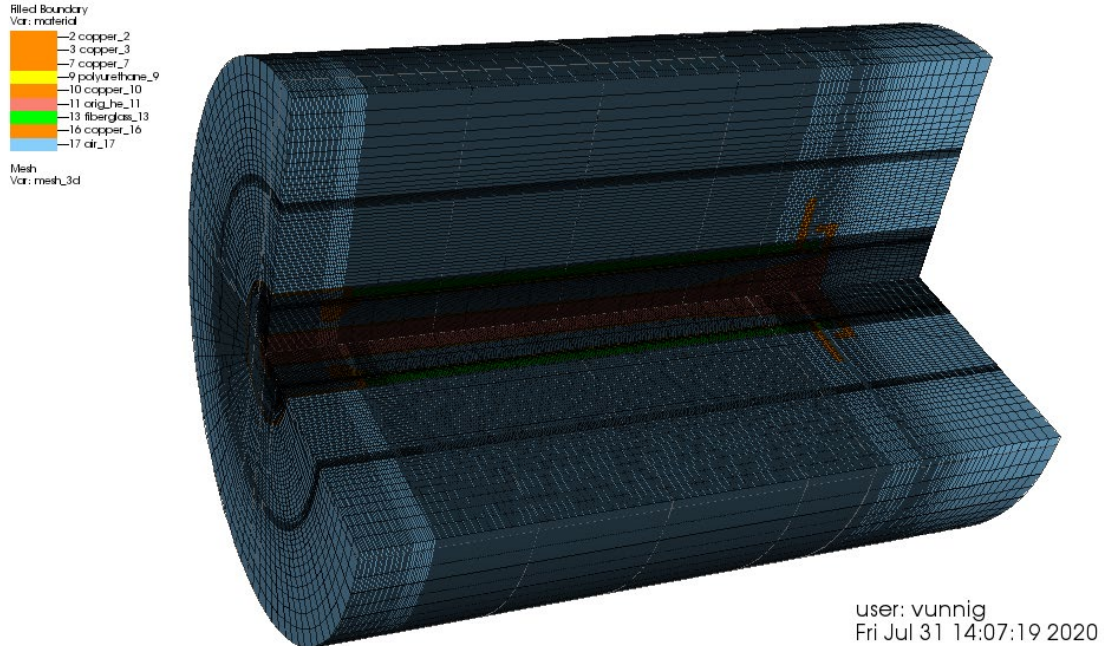


**Fig. 4 Computational mesh and simulation domain with 90° slice removed**

The simulation was constructed using graded 3-D cylindrical mesh. In ALE3D, a cylindrical mesh begins with a deformed block core. The nodes of the core (the center part of the cylinder inside the first radial stratum) are moved to an optimal location, and a radial (bands extending out radially from the axis) stratum (cross sections extending up along the axis) of elements is used to transition between the internal deformed block to the outer cylindrical surface. The entire domain shown in Fig. 4 contained 6.3 million elements and 13 materials regions.

Materials were inserted by shaping the cubic material geometries onto the ALE3D internal mesh. There are two broad approaches to modeling in ALE3D. A mesh that conforms to the structural elements in the system generally gives the most accurate simulation, but creating this type of mesh can be time-consuming. Since FCGs have a cylindrical geometry, a high-resolution mesh is not required; one can use a conformal mesh and paint (shape) the actual geometries onto the mesh, allowing mesh elements to intersect the user-defined shape. The mesh was defined by a built-in function of ALE3D. The mesh was constructed such that the stator (coil), the thinnest material, was highly resolved with approximately six elements across. Figure 5 shows the mesh of the FCG and a zoomed section of the stator (coil) showing six elements across the thickness.

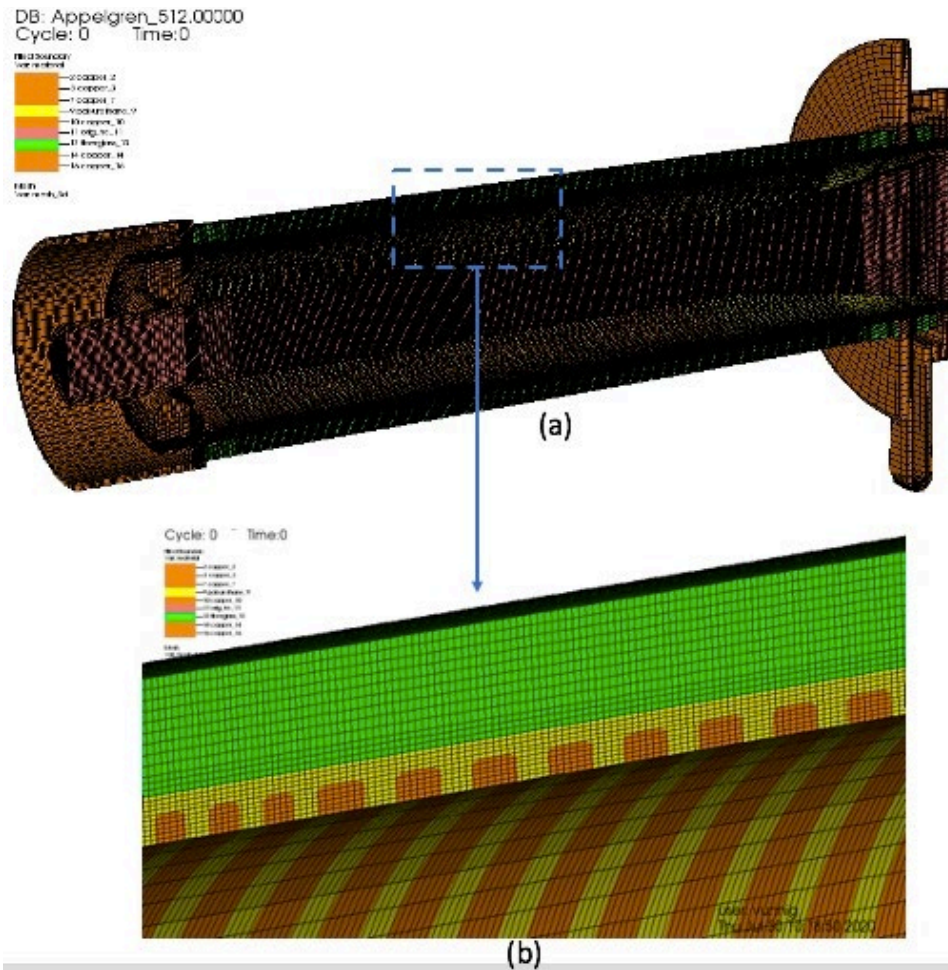


Fig. 5 a) Mesh of the FCG device and b) zoomed-in section of the FCG coil showing the number of elements

## 4.2 ALE3D Circuit Simulation Setup

Figure 6 shows the circuit network setup used in the ALE3D simulation. The seed current was supplied by an external seed capacitor bank and transmission line. The parameters of the experimental feed circuit were determined to be  $L = 900.0$  nH,  $C = 67.0$   $\mu$ F, and  $R = 85.0$  m $\Omega$  from the experimental data reported in Appelgren.<sup>1,2</sup> The capacitor charge voltage was 4.2 kV for FCG #1 and 8.0 kV for FCG #2 to give the correct seed current peaks reported in the experimental measurements. To disconnect the capacitor from the generator at crowbar time to divert the seed current, a large resistor of 100.0  $\Omega$  was placed in parallel with the generator during the simulation. The simulation was ran on 512 cores, with approximately 24 h of run time.

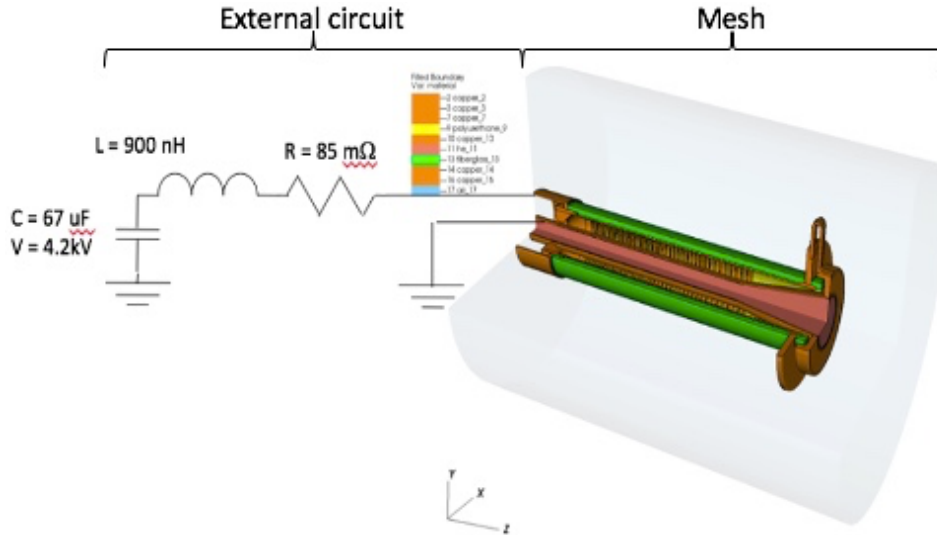


Fig. 6 ALE3D simulation setup showing the external circuit and the computational mesh

### 4.3 Material Properties

The copper conductor materials were modeled using SESAME equation of state (EOS) number 29333 and electrical conductivity tables based on the modified Lee–More conductivity model.<sup>8</sup> The explosive driving the armature, PBXN-5, was modeled using a Jones–Wilkins–Lee line-of-sight lighting model.<sup>9</sup> The air background was modeled with a simple gamma law gas EOS with a constant electrical conductivity. The detonation time ( $t = 50.0 \mu\text{s}$ ) was tuned to crowbar at approximately the same time as in the experiment reported in Appelgren.<sup>1</sup> Symmetry and magnetic boundary conditions were applied at  $z = 0$ . The hydrodynamic conditions at the outer boundaries allow outflow of material. Substantial amounts of material outflow occur late in time near the input end of the mesh.

## 5. ALE3D-MHD Simulation Results

ALE3D-MHD simulations using the setup described in Fig. 6 were run to a simulation time of approximately  $90 \mu\text{s}$  on 512 processors. The compressed current diagnostics are critical for comparing the simulation results with the experiment. It is one of the most important quantities of the simulation to predict magnetic compression in the FCG discharge. In the simulation, the current was measured by introducing a  $360^\circ$  ring of B-field tracers around the output reported in Vunni et al.<sup>4,5</sup> The orientation was such that B-field tracers follow the direction of the magnetic field along the vector line of the ring allowing it to measure accurately the compressed current.

From the generated time histories of the magnetic field  $B$ , the current was calculated at each time step by application of Ampere's law, integrating around the loop described by the tracers. As previously described, the explosive was initiated such that the modeled crowbar time corresponded to the experimental crowbar time. The dynamics of the simulation at this point are shown in Figure 7a. The geometry of the FCG after crowbar is shown in Figure 7b–e.

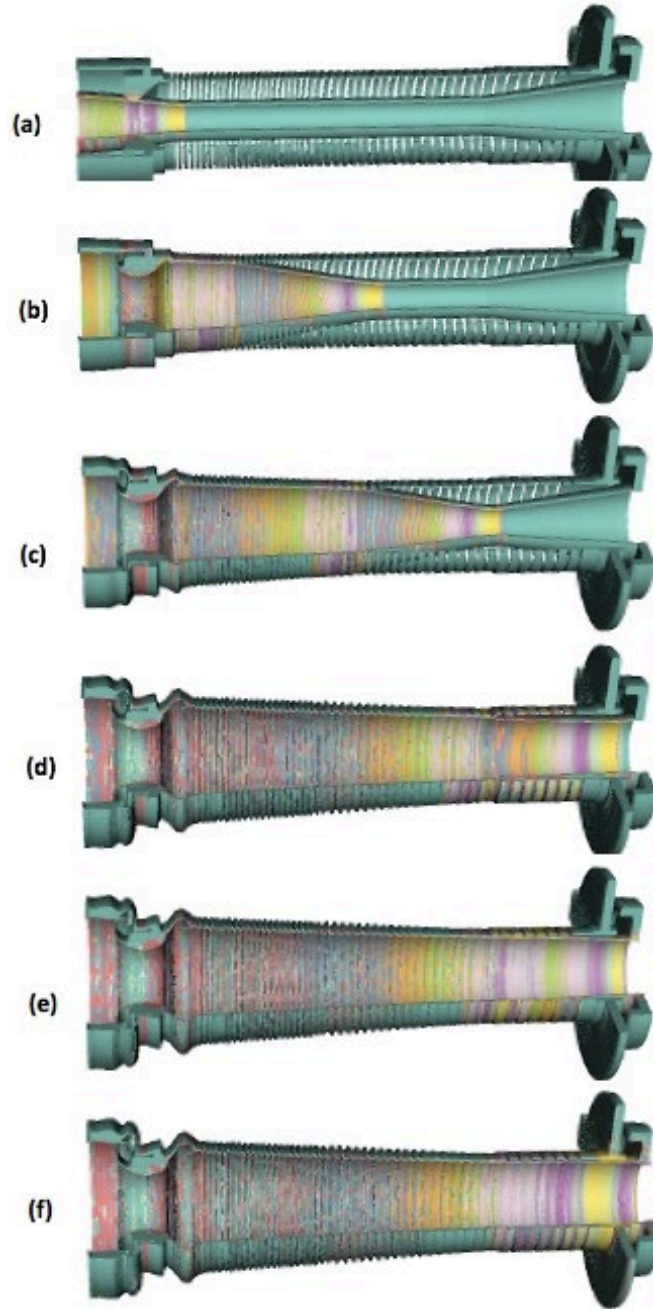


**Fig. 7** ALE3D simulation geometry at a) crowbar time, b) end of section 1, c) end of section 2, d) end of section 3, e) end of section 4, and f) end of compression

Figure 8 shows the seed current and load current at the generator output side for FCG #1 and FCG #2 from the ALE3D simulations and experiments. The agreement between the simulation and experiment is fairly reasonable for FCG #1 and differs slightly for FCG #2 at earlier times.

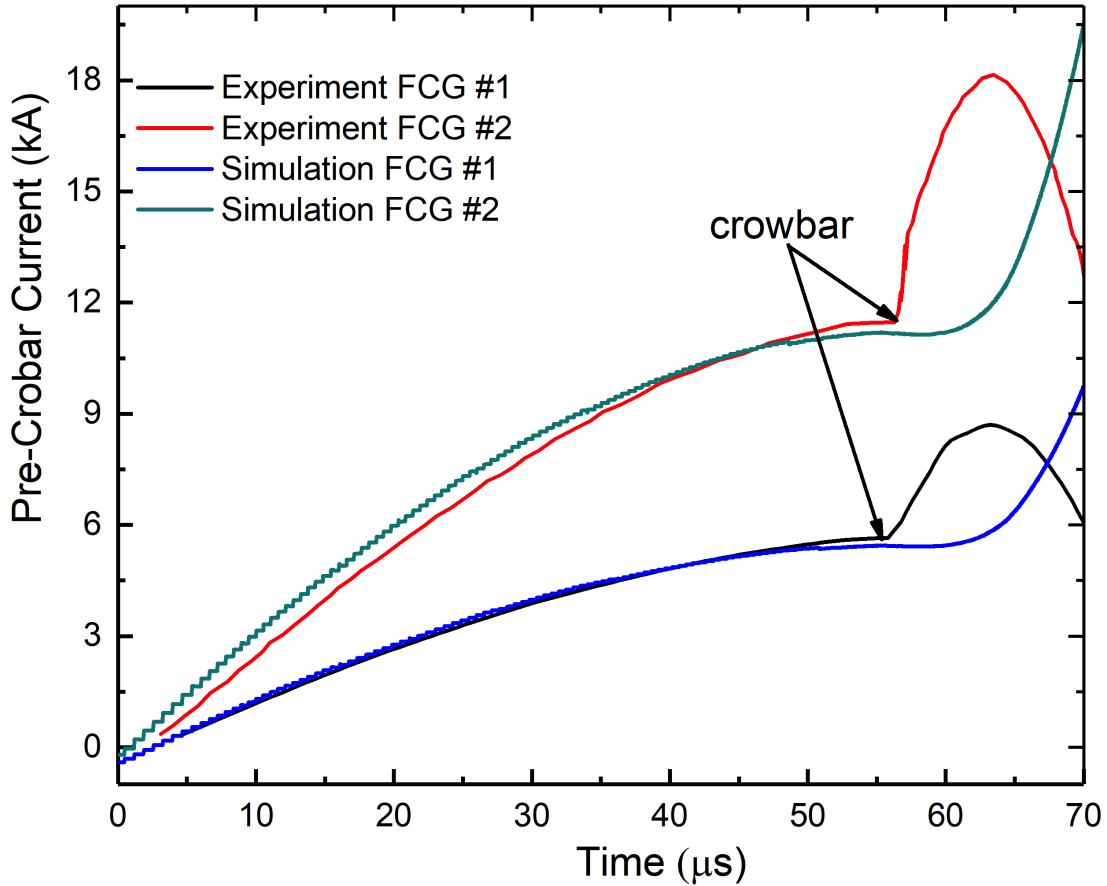


**Fig. 8** Pre-crowbar current plot from ALE3D simulation vs. experiment for FCG #1 and FCG #2

One obvious difference between the waveforms (FCG #2) in Fig. 8 is the capacitor charge voltage that was not explicitly reported in Appelgren’s work.<sup>1</sup> In addition, the experimental measurement at high frequency is not captured in the simulation.<sup>1-4</sup> It should be pointed out that after 6.5-μs initiation of the explosive, the armature makes contact with the crowbar, and it takes another 5.0 μs before the armature contacts the first stator turn. During this phase, the current will flow through the electrical circuit composed of the stator, the load, and armature with no flux compression taking place. At the same time, the external seed current is discharged through the crowbar short with no more impact on the current flow in the FCG. However, in Appelgren’s work (see Figs. 1 and 8), there appears a flux compression taking place after the crowbar, resulting in the rise of the seed current.

Figure 9a–b shows the experimental and simulation current post-crowbar. In these plots, the simulation and the experimental data have been shifted later in time (post-crowbar). The simulation lines up reasonably well during most of the generator operation, but overshoots the experiment at the end of the compression phase in both cases. For FCG #1 (5.7-kA seed current), the simulation predicted a maximum current of 330 kA, which differs from the measured peak current of 269 kA by approximately 61 kA at the end compression. For FCG #2, (11.2-kA seed current), the simulation predicted a maximum current of 540 kA, 104 kA higher than the measured value of 436 kA. In both configurations, ALE3D predicted a final current that exceeds the experimental data.

The overprediction in the simulation at the end of the compression (see Fig. 3, end of section 3 and section 4), may be due to losses in the experiment that are not captured by the simulation. One likely source of this difference could be that the skin depths in the copper conductors are under resolved. Increased mesh resolution may cause the current density to further concentrate near the surface of the coils and armature and therefore increase the overall losses. Future work may be investigating the effect of mesh resolution on the magnetic losses.

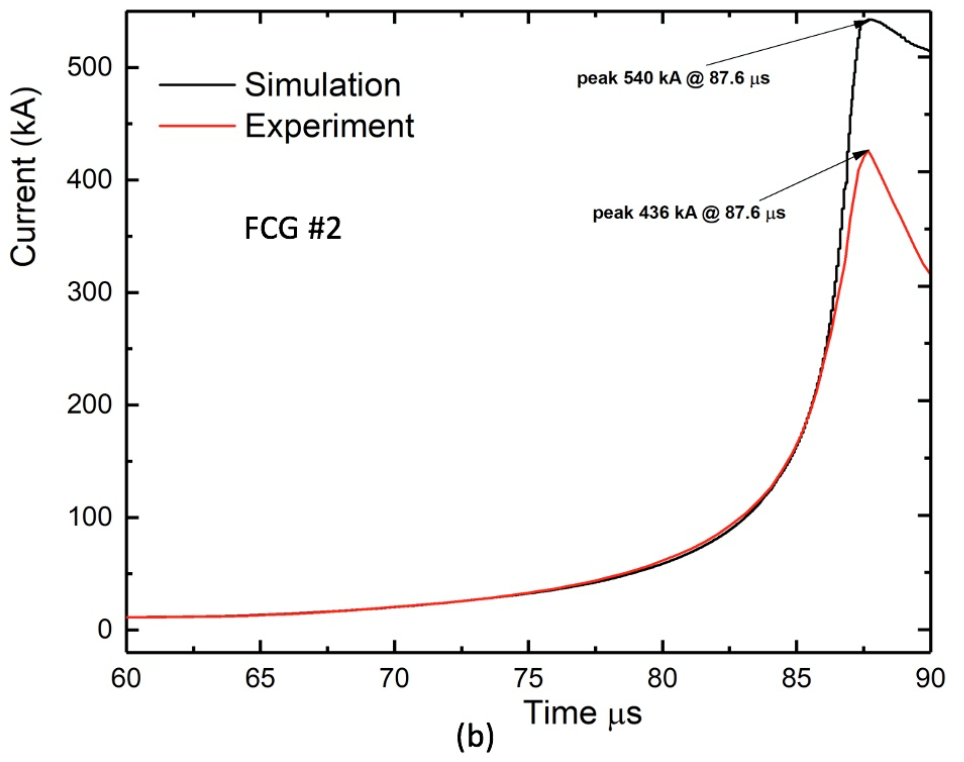
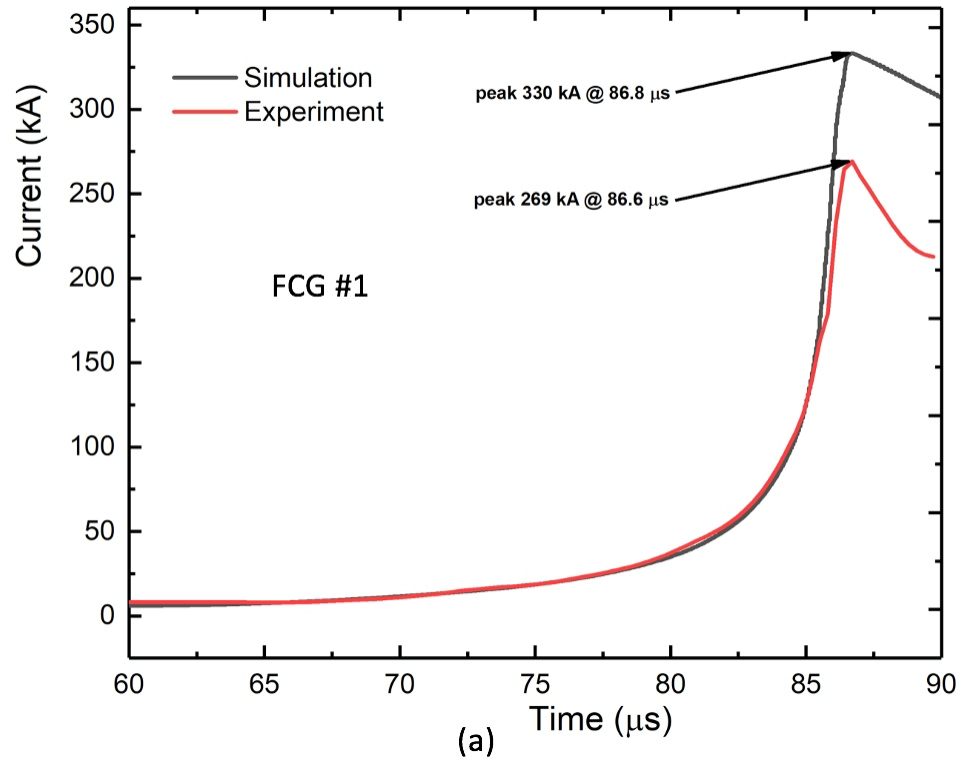


Fig. 9 ALE3D MHD current vs. experiment: a) FCG #1 and b) FCG #2

Another possible source of error in the difference between the simulation and experiment may be missing physics in the MHD model. A typical example of this is plasma creation near the contact point due to breakdown of the gas/insulators at the end of the compression. The ALE3D-MHD code used in this simulation is currently incapable of modelling this phenomenon in a predictive way. In the future, we may try to exercise the phenomenological breakdown models that have been recently implemented in ALE3D to address some of this issues. Notwithstanding of the sources of the error, the difference between the simulation and experiment at the end of the compression are small and the predictive capability of ALE3D appears to be very good for the operating regime of the FCG.

Figure 10 shows the plot of the time history of the inductance from FCG #1 during pre- and post-crowbar. The experimental data are included for comparison. The inductances calculated from the ALE3D simulations shows a very good agreement with the measured values. The experimental data were recorded after the crowbar, approximately 56.5  $\mu\text{s}$  after denotation. The measured inductance at crowbar is 22.3  $\mu\text{H}$ , similar to the ALE3D simulation. At a later time at the end of compression, the agreement with the experiment shows a final inductance of 0.3  $\mu\text{H}$ .

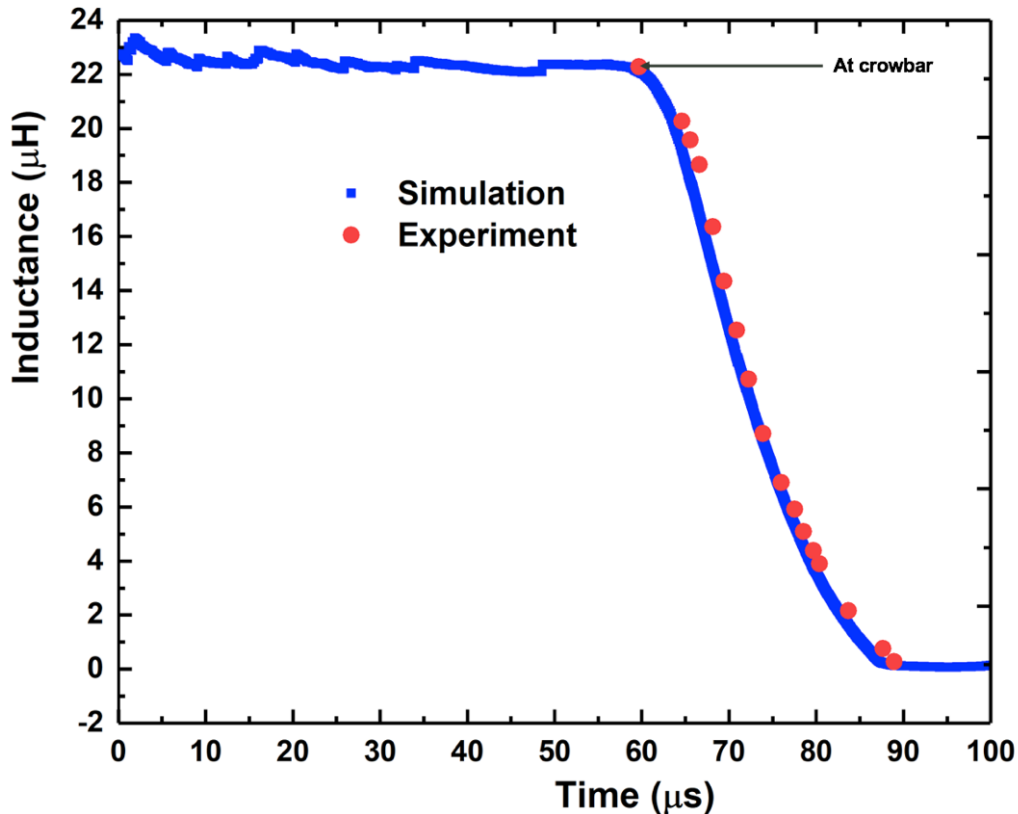


Fig. 10 ALE3D MHD inductance vs. experiment for FCG #1

## 6. Conclusion

---

A complete numerical simulation of Appelgren's FCG was investigated using the ALE3D-MHD shock physics code for two seed currents. The results demonstrate that ALE3D-MHD provides a reasonable prediction of the FCG operation. For 5.7-kA seed current (FCG #1), the compressed current was 330 kA. For the 11.2-kA seed current (FCG #2), the measured maximum current was 436 kA compared to the simulated current of 540 kA. Clearly, the experimental comparison considered in this work shows that MHD analysis can be used for quantitative predictive analysis of helical FCGs. The experiment used in this work at higher seed current (FCG #2) may have exhibited increased losses due to ohmic heating, magnetic pressure, and possible electrical breakdown. While ALE3D-MHD code cannot predict the electrical breakdown component or nonlinearity in the conductivity model, it does appear to approximately capture the flux compression during the operation for the FCG.

Improvements upon this work may consider using the electrical breakdown model and a more comprehensive set of simulations on a finer mesh. However, the current simulations pave the way for further work to model and improve similar CCDC Army Research Laboratory FCG designs. Improved electrical conductivity models could also prove helpful as new FCG designs are built and tested.

## 7. References

---

1. Appelgren P. Experiments with and modeling of explosively driven magnetic flux compression generators. [thesis] [Stockholm (Sweden)]: School of Electrical Engineering Space and Plasma Physics Royal Institute of Technology; 2008.
2. Appelgren P, Brenning N, Hurtig T, Larson A, and Novac B. Modeling of a small helical magnetic flux-compression generator. *IEEE Trans Plasma Sci.* 2008 Oct;36(5).
3. Appelgren P, Bjarnholt G, Brenning N, Elfsberg M, Hurtig T, Larson A, Novac B. Small helical magnetic flux compression generators: experiments and analysis. *IEEE Trans Plasma Sci.* 2008 Oct;36(5).
4. Appelgren P, Bjarnholt G, Brenning N, Elfsberg M, Hurtig T, Larson A, Nyholm SE. Analysis of experiments with small helical magnetic flux compression generators. Eleventh International Conference on Megagauss Magnetic Field Generation and Related Topics (MG-XI); 2006 Sep 10–14; Imperial College, London, UK:
5. Vunni GB, Bartkowski P, Johnson A. ALE3D magneto-hydrodynamic (MHD) modeling of a new ARL squeeze 5 magnetic flux compression generator. Aberdeen Proving Ground (MD): Army Research Laboratory (US); 2018 Sep. Report No.: ARL-TR-8505.
6. Vunni GB. Magneto-hydrodynamic simulations of a magnetic flux compression generator using ALE3D. Aberdeen Proving Ground (MD): Army Research Laboratory (US); 2017 July. Report No.: ARL-TR-8055.
7. Bartkowski P, Berning P. Design and testing of the ARL squeeze 4 helical flux compression generator. Aberdeen Proving Ground (MD): Army Research Laboratory (US); 2013 June. Report No.: ARL-TR-6477.
8. Desjarlais MP. Practical improvements to the Lee-More conductivity near the metal-insulator transition. *Contributions to Plasma Physics.* 2001;41:267–270.
9. Anderson A, Barton N, Biagas K. User manual for ALE3D, an arbitrary Lagrange Eulerian system, version 4.24. Livermore (CA): Lawrence Livermore National Laboratory; 2014 Sep 5.

## List of Symbols, Abbreviations, and Acronyms

---

ALE	arbitrary Lagrangian–Eulerian
CCDC	US Army Combat Capabilities Development Command
EOS	equation of state
FCG	flux compression generator
FOI	Swedish Defense Research Agency
MHD	magnetohydrodynamic

1 DEFENSE TECHNICAL  
(PDF) INFORMATION CTR  
DTIC OCA

E KLIER  
K KRAUTHAUSER  
P SWOBODA

1 CCDC ARL  
(PDF) FCDD RLD DCI  
TECH LIB

2 SANDIA NATL LAB  
(PDF) J NIEDERHAUS  
A E RODRIGUEZ

1 LAWRENCE LIVERMORE  
(PDF) NATL LAB  
A J JOHNSON

37 CCDC ARL  
(PDF) FCDD RLW B  
R BECKER  
C HOPPEL  
FCDD RLW C  
P BARTKOWSKI  
FCDD RLW P  
R FRANCAERT  
FCDD RLW PA  
P BERNING  
S BILYK  
M COPPINGER  
J FLENIKEN  
M GREENFIELD  
W UHLIG  
FCDD RLW PD  
A BARD  
S BOYER  
N BRUCHEY  
R DONEY  
M KEELE  
D KLEPONIS  
B KRZEWINSKI  
K MASSER  
F MURPHY  
C RANDOW  
S SCHRAML  
K STOFFEL  
G VUNNI  
V WAGONER  
M ZELLNER  
B LINNE  
D WEBB  
R GUPTA  
N BERARDI  
M DEVINE  
E ELDRIDGE  
FCDD RLW PE  
D GALLARDY  
D HORNBAKER